Heating dynamics of bosonic atoms in a noisy optical lattice

Hannes Pichler,[1,2] Johannes Schachenmayer,[1,2,3] Andrew J. Daley,[3] and Peter Zoller[1,2]
[1]*Institute for Theoretical Physics, University of Innsbruck, A-6020 Innsbruck, Austria*
[2]*Institute for Quantum Optics and Quantum Information of the Austrian Academy of Sciences, A-6020 Innsbruck, Austria*
[3]*Department of Physics and Astronomy, University of Pittsburgh, Pittsburgh, Pennsylvania 15260, USA*
(Received 13 January 2013; published 5 March 2013)

We analyze the heating of interacting bosonic atoms in an optical lattice due to intensity fluctuations of the lasers forming the lattice. We focus in particular on fluctuations at low frequencies below the band-gap frequency, such that the dynamics is restricted to the lowest band. We derive stochastic equations of motion, and analyze the effects on different many-body states, characterizing heating processes in both strongly and weakly interacting regimes. In the limit where the noise spectrum is flat at low frequencies, we can derive an effective master equation describing the dynamics. We compute heating rates and changes to characteristic correlation functions both in the perturbation theory limit and using a full time-dependent calculation of the stochastic many-body dynamics in one dimension based on time-dependent density-matrix–renormalization-group methods.

DOI: 10.1103/PhysRevA.87.033606 PACS number(s): 67.85.Hj, 37.10.Jk, 42.50.−p

I. INTRODUCTION

Ultracold atoms in optical lattices provide a clean and controllable realization of quantum dynamics of an isolated many-body system on a lattice [1–3]. The remarkable progress in optical lattice physics is underlined by recent experiments including the quantitative determination of phase diagrams and critical phenomena of strongly interacting Hubbard models [4–11], studies of quantum magnetism [12], and nonequilibrium quench dynamics [13–15]. A basic experimental challenge is the preparation of low entropy or low-temperature states in optical lattices, and to avoid possible heating mechanisms [7,13,14]. Heating can either be due to fundamental decoherence sources like spontaneous emission [16–19], or collisional losses [20–22], and also due to technical noise, for example, amplitude or phase noise of the lasers [23] generating the optical lattice. While in a recent publication [24] we have described possible optical lattice schemes which are immune to laser intensity fluctuations, we will present below a detailed study of heating of bosonic atoms in an optical lattice as a many-body nonequilibrium problem.

We will study below heating within a *single band Bose-Hubbard model* where the tunneling and hopping parameters are stochastic functions of time reflecting the intensity noise of the laser. We derive this model under the assumption that the noise spectrum contains only significant components below the band gap of the lattice, i.e., noise induced transitions to higher bands can be neglected. In our model the intensity fluctuations of the light act as a *global noise*, which corresponds to the assumption that the spatial correlations of the laser fluctuations are certainly much larger than the size of the atomic cloud. The resulting stochastic Schrödinger equation for the Bose-Hubbard dynamics will be solved in detail in various limits and approximations. First, we will compute the heating rates and the time dependence of characteristic correlation functions in a perturbative calculation valid for short times. In the white-noise limit for the intensity fluctuations we will be able to perform the stochastic average and derive a master equation for the many-particle systems containing both the Hubbard dynamics and the heating terms. In addition, we will solve the stochastic many-body Schrödinger equation in a Gutzwiller mean-field approximation, and in one dimension with a time-dependent density-matrix–renormalization-group (t-DMRG) technique as a multiplicative stochastic differential equation. Besides computing the total average energy transfer to the system as part of the heating dynamics, we will also provide a detailed study of the excitations in the many-body system as signatures of the applied noise.

The paper is organized as follows. In Sec. II we derive a stochastic Schrödinger equation for cold atoms in an optical lattice in the presence of intensity noise. In Sec. II C we describe the methods we use to analyze the resulting nonequilibrium dynamics, including full time-dependent calculations based on t-DMRG calculations in one dimension (1D) and a Gutzwiller mean-field approach for three-dimensional (3D) lattices. In Sec. III we present the resulting time-dependent dynamics and discuss heating in different parameter regimes, and in Sec. IV we present a summary and outlook.

II. STOCHASTIC MANY-BODY SCHRÖDINGER EQUATION

In this section, we derive and discuss a stochastic many-body Schrödinger equation (SMBSE) for ultracold bosonic atoms in an optical lattice in the presence of intensity fluctuations of the laser generating the lattice. We are interested in a situation where the atoms in the optical lattice are prepared in the lowest Bloch band with dynamics described by a single band Bose-Hubbard model [25],

$$H(J,U) = -J\sum_{\langle i,j\rangle} b_i^\dagger b_j + \frac{U}{2}\sum_i b_i^\dagger b_i^\dagger b_i b_i. \qquad (2.1)$$

Here the hopping amplitude and on-site interaction energy are denoted by J and U respectively. The operators b_i are the annihilation operators for particles at site i. For deep lattices simple arguments give the dependence $J \sim \frac{4}{\sqrt{\pi}} E_R (V/E_R)^{3/4} \exp(-2\sqrt{V/E_R})$ and $U \sim 8E_R(V/E_R)^{3/4}$ on the depth V of the optical lattice (with E_R being the lattice recoil energy). Thus an increase of the lattice depth V suppresses the tunneling, while at the same time the on-site interaction becomes larger (Fig. 1). The single-band

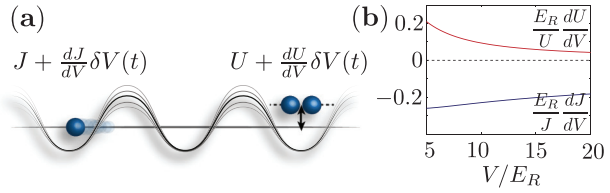

FIG. 1. (Color online) (a) We consider bosons in an optical lattice where noise in the lattice depth leads to noise in the hopping amplitude and in the interaction energy. (b) Relative change of the hopping and the interaction parameter with lattice depth in an isotropic three-dimensional cubic optical lattice, generated in the standard way by three counterpropagating laser beams. Note that the change in the hopping and interaction parameter is anticorrelated in this setup.

tight-binding model is valid provided the on-site interaction and temperature are much lower than the gap to the first excited band.

Laser intensity noise can be included in the Bose-Hubbard dynamics as $V(t) = V_0 + \delta V(t)$ with $\delta V(t)$ fluctuations around the mean lattice depth V_0. For small fluctuations the tunneling $J(t) = J_0 + \frac{dJ}{dV}\delta V(t)$ and on-site interaction $U(t) = U_0 + \delta V(t)\frac{dU}{dV}$ will become stochastic variables (see Fig. 1), and we can write a stochastic many-body Schrödinger equation (SMBSE) ($\hbar = 1$)

$$\frac{d}{dt}|\Psi\rangle = -i\left[H(J_0,U_0) + H\left(\frac{dJ}{dV},\frac{dU}{dV}\right)\delta V(t)\right]|\Psi\rangle \equiv -i[H + H'\delta V(t)]|\Psi\rangle, \tag{2.2}$$

for a given noise model $\delta V(t)$. The derivatives $\frac{dJ}{dV}$, $\frac{dU}{dV}$ are evaluated at V_0 such that $H \equiv H(J_0,U_0)$ and $H' \equiv H(\frac{dJ}{dV},\frac{dU}{dV})$ are time independent. While H induces coherent evolution according to the standard Bose-Hubbard Hamiltonian, H' describes the heating in the lowest lattice band due to intensity noise. We expect the above model to be valid provided the fluctuation spectrum of $\delta V(t)$ is narrow on the scale given the separation to the first Bloch band. Otherwise, the noise will excite atoms to the higher Bloch bands.

While the above heuristic derivation is intuitively obvious, we summarize below in Sec. II A a rigorous derivation of the above model starting from a multiband Hubbard model, which establishes the validity of the SMBSE given above, and gives corrections due to interband transitions. In Sec. II B we will discuss the derivation of a master equation for the averaged density operator $\rho(t) = \langle\langle|\Psi(t)\rangle\langle\Psi(t)|\rangle\rangle$ with $\langle\langle\ldots\rangle\rangle$ denoting a stochastic average over the noise. This is possible under the assumption of a white-noise limit, i.e., $\delta V(t)$ is modeled by Gaussian white noise (within the single band model). In Sec. II C we will discuss mean-field and DMRG versions of the SMBSE, and their simulation.

Finally we note that similar discussions can be found in work on lattice spectroscopy [26–31]. There the potential is not fluctuating stochastically but modulated periodically in time.

A. Bose-Hubbard model with intensity noise

To derive Eq. (2.2) We consider atoms (of mass m) in an optical potential $V_{\rm opt}(x) = [V_0 + \delta V(t)]\sin^2(kx)$, which for simplicity of notation we assume to be one dimensional. Here k is the wave vector of the laser generating the lattice, which is related to the lattice constant a via $a = \pi/k$ and sets an energy scale via the recoil energy $E_R = k^2/(2m)$. The full many-body Hamiltonian can be written in second quantization using the bosonic field operators $\hat\psi(x)$ [$\hat\psi^\dagger(x)$] that destroy (create) a particle at the position x as

$$H(V(t)) = \int dx\, \hat\psi^\dagger(x)\left(-\frac{1}{2m}\frac{d^2}{dx^2} + V(t)\sin^2(kx)\right)\hat\psi(x) + \frac{g}{2}\int dx\, \hat\psi^\dagger(x)\hat\psi^\dagger(x)\hat\psi(x)\hat\psi(x), \tag{2.3}$$

where $g = 4\pi\hbar^2 a_s/m$ and a_s is the s-wave scattering length.

We are interested in the limit where the stochastic $\delta V(t)$ is much slower than the (fast) time scale associated with the band gap. For a given lattice depth V the Wannier states $w_{j,n}(x,V)$ form a complete basis. Thus it is natural to employ an adiabatic (Born-Oppenheimer) picture, where field operators are expanded into *instantaneous* Wannier states, that is $\hat\psi(x) = \sum_{i,n} w_{j,n}(x,V(t))b_{i,n}(V(t))$, where $b_{i,n}(V(t))$ annihilates a boson in the instantaneous Wannier state $w_{j,n}(x,V(t))$ at site i in band n. In this way the single-particle basis states keep track of variations of $V(t)$ on a slow time scale. Nonadiabatic transitions due to the time dependence of the basis states are driven by fast changes in the lattice potential. As shown in the Appendix the coefficients of the wave function $|\Psi\rangle$ in the time-dependent Fock basis corresponding to this instantaneous Wannier states, $\langle\{n_{i,n}\}|\Psi\rangle$, evolve according to

$$i\frac{d}{dt}\langle\{n_{i,n}\}|\Psi\rangle = \langle\{n_{i,n}\}|H(V(t)) + G(V(t))\dot V(t)|\Psi\rangle,$$

with

$$H(V) = -\sum_n J_n(V)\sum_{\langle i,j\rangle} b^\dagger_{i,n}b_{j,n} + \sum_{n,i}\varepsilon_n(V)b^\dagger_{i,n}b_{i,n} + \frac{1}{2}\sum_i\sum_{\{n\}} U_{\{n\}}(V)b^\dagger_{i,n_1}b^\dagger_{i,n_2}b_{i,n_3}b_{i,n_4}, \tag{2.4}$$

$$G(V) = i\sum_{i,n;j,m}\int dx\, w_{j,m}(x,V)\frac{dw_{i,n}(x,V)}{dV}b^\dagger_{i,n}b_{j,m}. \tag{2.5}$$

To simplify notation we suppressed the explicit dependence of the bosonic operators and the Fock basis states on the instantaneous lattices depth $V(t)$. An independent derivation and discussion of this equation in the context of a deterministically modulated lattice depth can be found in [31].

Due to the localized nature of the Wannier functions only nearest-neighbor hopping and on-site interactions are considered in (2.4). The first term (2.4) is simply the multiband Bose-Hubbard Hamiltonian with time-dependent parameters, corresponding to the time-dependent lattice depth. The second term in (2.5) arises from the time dependence of the basis we use to describe the system. It is proportional to the time derivative of the potential depth. In the Appendix we give a detailed discussion of this term and we show that it drives transitions between different bands, but does not couple states within the same band. More precisely, this *interband* term mainly couples atoms to the second excited band such that the number of atoms in the lowest band N_0 decreases in time as $\dot N_0/N_0 \approx -2\eta^4 S_2$. Here S_2 is the noise spectrum at the transition frequency from the lowest to the second excited band and $\eta = \pi a_0/a \lesssim 0.1$ is the Lamb-Dicke parameter that

compares the extension a_0 of the lowest band Wannier function to the lattice constant a. This sets the time scale on which the restriction to the lowest band is valid. For fluctuations that are slow on the time scale of the gap this term is off resonant and can be dropped.

Under the same constraints also the first term in (2.4) can be restricted to the lowest band and by linearizing the dependence of $J(V)$ and $U(V)$ for small fluctuations on finds Eq. (2.2). In the following we will describe the heating dynamics on the basis of the single band model (2.2).

B. White-noise approximation and master equation

We are interested in calculating the response of the many-body system to the noise stochastically averaged over the various realizations of $\delta V(t)$. This stochastic averaging can be performed exactly if we make the assumption of white noise $\langle\langle \delta V(t)\delta V(t')\rangle\rangle = S_0\delta(t-t')$. We note that this white-noise approximation implies that the fluctuations of $\delta V(t)$ are much faster than $1/J$ and $1/U$, but are much slower than the transition frequency to the first excited band. We can thus write the SMBSE as a Stratonovich stochastic differential equation

$$(S)\quad d|\Psi\rangle = -iH|\Psi\rangle dt - iH'\sqrt{S_0}|\Psi\rangle dW_t, \tag{2.6}$$

where S_0 denotes the strength of the noise and dW_t is a Wiener increment [32,33]. This is a multiplicative differential equation, for which the averaging over the noise can be performed exactly to derive a (master) equation for $\rho = \langle\langle|\Psi\rangle\langle\Psi|\rangle\rangle$.

To derive the master equation for ρ, we find it convenient to transform the above equation to an Ito equation,

$$(I)\quad d|\Psi\rangle = \left(-iH - \frac{S_0}{2}H'^2\right)|\Psi\rangle dt - iH'\sqrt{S_0}|\Psi\rangle dW_t.$$

Using the Ito rules for stochastic calculus [32,33] one finds the following many-body master equation:

$$\frac{d}{dt}\rho = -i[H,\rho] - \frac{S_0}{2}[H',[H',\rho]]. \tag{2.7}$$

We note that this equation is of Lindblad form. The first term on the right-hand side is the familiar Bose-Hubbard Hamiltonian (2.1), while the second term describes heating. We note that the assumption of global intensity noise is reflected in the *spatially nonlocal* heating terms contained in the double commutator. The above equation is derived from averaging over classical noise (as opposed to coupling to a quantum reservoir). As a consequence solutions $\rho(t)$ will in general approach for long times $\rho \sim \hat{1}$ corresponding to an (infinite temperature) completely mixed state (within the subspace allowed by the conserved quantities).

In Sec. III below we will derive analytical, perturbative solutions of the master equation to describe the initial heating of a many-body quantum state in the limit of weak ($U \ll J$) and strong interactions ($U \gg J$). However, for general parameters we find it more convenient instead of solving the master equation numerically to compute averages from simulating trajectories of SMBSE (cf. Sec. II C).

C. Simulation of the stochastic many-body Schrödinger equation

A simulation of the SMBSE as a multiplicative stochastic differential equation can be performed in a mean-field limit and for 1D systems using t-DMRG techniques [34–37] or exact state representation for small systems.

The (mean field) Gutzwiller-ansatz [38–40] for the Bose-Hubbard model relies on a product state assumption $|\Psi\rangle = \prod_l |\phi_l\rangle = \prod_l \sum_n f_{l,n}|n\rangle_l$. The time-dependent variational ansatz [41,42] for a homogeneous system leads to a nonlinear Stratonovich stochastic Schrödinger equation of the form

$$(S)\quad d|\phi_l\rangle = -iH_l|\phi_l\rangle dt - i\sqrt{S_0}H_l'|\phi_l\rangle dW, \tag{2.8}$$

where

$$H_l = -zJ(\psi_l^* b_l + \psi_l b_l^\dagger) + \frac{U}{2}b_l^{\dagger 2}b_l^2, \tag{2.9}$$

$$H_l' = -z\frac{dJ}{dV}(\psi_l^* b_l + \psi_l b_l^\dagger) + \frac{1}{2}\frac{dU}{dV}b_l^{\dagger 2}b_l^2, \tag{2.10}$$

and $\psi_l = \langle\phi_l|b_l|\phi_l\rangle$. The number of nearest neighbors is denoted by z.

To simulate the stochastic differential equation we typically used a semi-implicit method given in [33] of strong order 1.0. The evolution in a small time step Δt is calculated from

$$\begin{aligned} |\bar{\Psi}_t\rangle &= |\Psi_t\rangle - \frac{i}{2}H|\bar{\Psi}_t\rangle\Delta t - \frac{i}{2}\sqrt{S}H'|\bar{\Psi}_t\rangle\Delta W, \\ |\Psi_{t+\Delta t}\rangle &\approx 2|\bar{\Psi}_t\rangle - |\Psi_t\rangle, \end{aligned} \tag{2.11}$$

with a randomly chosen Wiener increment chosen from a normal distribution $\Delta W = W(\Delta t) - W(0) \sim \mathcal{N}(0,\Delta t)$. The density matrix and expectation values of operators are then obtained by averaging over the trajectories calculated in this way. We directly incorporate this propagation scheme for exact state representations and the analog version for the Gutzwiller equations (2.8).

Similar techniques can be employed in t-DMRG. There it is more convenient to implement the propagation step in the form of a Trotter decomposition. Therefore, we write the 1D Hamiltonian and noise term as sum over next-neighbor operators $H = \sum_i H_{i,i+1}$ and $H' = \sum_i H'_{i,i+1}$, respectively. For small time steps the evolution step can then be implemented as

$$|\Psi_{t+\Delta t}\rangle \approx \prod_i e^{-i\Delta t H_{i,i+1}} \prod_i e^{-i\Delta W H'_{i,i+1}}|\Psi_t\rangle. \tag{2.12}$$

To lowest order this is equivalent to the Euler algorithm and of weak order 1.0 convergence [32,33]. Note that we did not find any stability issues when using a number conserving update of the matrix product states. We further confirmed that for sufficiently small time steps the results from the propagation (2.12) coincide with the results obtained by exact state representation from (2.11) for small systems (N bosons on M sites with $N = M \leqslant 10$).

III. NONEQUILIBRIUM MANY-BODY DYNAMICS AND HEATING

In this section we show our results for the heating rates and analyze how the noise changes the characteristics of the

many-body ground state in the system. We show how to obtain analytical results for heating rates in the two limiting cases of a weakly interacting condensate in the superfluid (SF) phase ($U \ll J$) and of a nearly perfect Mott insulator (MI) ($U \gg J$) and compare them to numerical simulations in Sec. III A. In Sec. III B we analyze how the noise changes the characteristics of the state and analyze the evolution of the condensate fraction.

A. Heating rates

If the density operator is diagonal in the eigenstates of the Hamiltonian $H = H_J + H_U$ (where H_J and H_U denote the kinetic- and interaction-energy terms in the Bose-Hubbard model), for example if the system is in the ground or a thermal state, the average increase of the energy $E = \langle H \rangle$ can be calculated from the master equation (2.7) and is

$$\langle\langle \dot{E} \rangle\rangle = \frac{S_0}{2}\left(\frac{1}{J}\frac{dJ}{dV} - \frac{1}{U}\frac{dU}{dV}\right)^2 \langle [[H_J, H_U], H_J] \rangle. \tag{3.1}$$

The expectation value can be evaluated analytically in the limiting cases of an ideal superfluid state, and an ideal Mott insulating state, as discussed below.

From (3.1) we see that the heating vanishes if

$$\frac{1}{J}\frac{dJ}{dV} = \frac{1}{U}\frac{dU}{dV}. \tag{3.2}$$

Only if this condition is met, the Hamiltonian H and the noise operator H' commute, moreover this means that they are proportional to each other. As a consequence all states that commute with H, such as energy eigenstates or thermal states, are stationary if (3.2) is satisfied (see Fig. 2). In the standard setup, the hopping rate always decrease with the lattice depth, while the on-site interaction always increases, such that there is no such "sweet spot" [see Fig. 1(b)]. However, one can come up with more elaborate lattice setups (see, for example, [24]) that

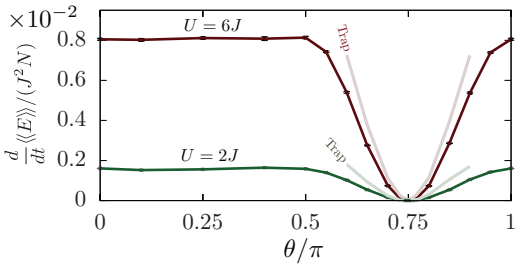

FIG. 2. (Color online) Short-time heating rates of superfluid ($U = 2J$) and Mott insulator states ($U = 6J$) in one dimension as a function of the relative magnitude of noise on J and U. We parametrize the correlations between the noise on J and U by θ and λ as $\sqrt{S}(dJ/dV)/J = -\lambda\cos^2(\theta)$ for $0 \leqslant \theta < \pi/2$; $\sqrt{S}(dU/dV)/U = \lambda\sin^2(\theta)$ and $\sqrt{S}(dJ/dV)/J = \lambda\cos^2(\theta)$ for $\pi/2 \leqslant \theta < \pi$. The usual anticorrelated case corresponds to $\theta < \pi/2$, and the sweet spot $\xi = 0$ of Eq. (3.2) to $\theta = 3\pi/4$. The heating rates are calculated from linear regression over 500 t-DMRG trajectories in a system with 30 particles on 30 sites (open boundary conditions). In both cases heating is strongly suppressed in the vicinity of the sweet spot. Thin lines show results in the presence of a harmonic trap with $\varepsilon_i/J = 0.0356 i^2$, $\sqrt{S_0}\frac{d\varepsilon_i}{dV}\frac{1}{\varepsilon_i} = 5\times 10^{-3} J^{-1/2}$; in both cases we used $\lambda = 0.02 J^{-1/2}$, time step $\Delta t = 10^{-2}/J$.

are designed in such a way to fulfill the sweet spot condition and therefore are resilient against this type of noise. For later convenience we introduce the parameter

$$\xi = \left(\frac{1}{U}\frac{dU}{dV} - \frac{1}{J}\frac{dJ}{dV}\right), \tag{3.3}$$

that measures the deviation from this sweet spot.

1. Weak interactions

If the interactions are weak, the ground state of the system is a Bose-Einstein condensate, where a macroscopic number of atoms occupies the mode with zero quasimomentum. For an ideal condensate we obtain from Eq. (3.1) (for a cubic lattice with z nearest neighbors and a filling of $\bar{n}$ atoms per site) to lowest order in U/J the heating rate per particle:

$$\frac{\langle\langle \dot{E} \rangle\rangle}{N} = S_0\left(\frac{1}{J}\frac{dJ}{dV} - \frac{1}{U}\frac{dU}{dV}\right)^2 zJU^2\bar{n}. \tag{3.4}$$

To find corrections to this result we can apply a Bogoliubov approximation. This approximation is most conveniently expressed in the Bloch basis rather than in the Wannier basis, such that the kinetic part of the Hamiltonian reads $H_J = \sum_q \varepsilon_q b_q^\dagger b_q$, where the single-particle energy spectrum ε_q for a cubic lattice in d dimensions is $\varepsilon_q = 2J\sum_{i=1}^d [1 - \cos(q_i a)]$. Here q_i denotes the component of the quasimomentum along direction i. The interaction is treated on a mean-field level, replacing $H_U \to U\bar{n}/2\sum_q (2b_q^\dagger b_q + b_q b_{-q} + b_q^\dagger b_{-q}^\dagger)$. The total Hamiltonian is then quadratic and can be diagonalized by a standard Bogoliubov transformation $b_q = u_q c_q + v_{-q} c_{-q}^\dagger$ such that $H = \sum_q \tilde{\varepsilon}_q c_q^\dagger c_q$, with $\tilde{\varepsilon}_q = \sqrt{\varepsilon_q(\varepsilon_q + 2U\bar{n})}$. Within the same approximation the noise operator $H' = \frac{1}{J}\frac{dJ}{dV}H_J + \frac{1}{U}\frac{dU}{dV}H_U$ is also quadratic. However, the Bogoliubov transformation diagonalizing H does not diagonalize H' [except if condition (3.2) is met]. Therefore, the noise operator contains terms $c_q^\dagger c_{-q}^\dagger$ and thus excites pairs of Bogoliubov excitations with opposite quasimomenta [Fig. 3(a)]. The total

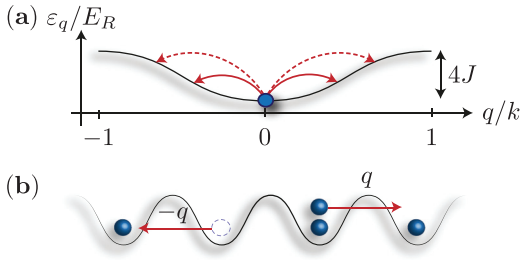

FIG. 3. (Color online) Elementary heating processes in the limiting cases of weak and strong interaction. (a) For weak interactions ($U \ll J$) lattice fluctuations create pairs of Bogoliubov excitations with opposite quasimomenta on top of the Bose-Einstein condensate at $q = 0$. (b) In the strongly interacting case ($U \gg J$) lattice fluctuations create pairs of excess particles and holes of opposite quasimomenta $\pm q$ on top of the Mott insulator.

quasimomentum is conserved as required by the conserved symmetry. The heating rate associated with this process can easily be calculated from (3.1) for the vacuum of quasiparticles. For a d-dimensional cubic lattice ($z = 2d$) it is given by

$$\frac{\langle\langle \dot{E} \rangle\rangle}{N} = S_0 \left(\frac{1}{J}\frac{dJ}{dV} - \frac{1}{U}\frac{dU}{dV} \right)^2 2JU^2 \bar{n} G(\bar{n}U/J), \tag{3.5}$$

with

$$G(\epsilon) = \frac{1}{\pi^d} \int_{0<x_i<\pi} d^d x \frac{\left(\sum_{i=1}^d [1-\cos(x_i)]\right)^{3/2}}{\left(\sum_{i=1}^d [1-\cos(x_i)] + \epsilon\right)^{1/2}}. \tag{3.6}$$

In one dimension this integral can be calculated exactly and leads to

$$G(\epsilon) = 1 - \frac{\epsilon}{2} + \frac{4}{\pi}\sqrt{\frac{\epsilon}{2}} + \frac{1}{\pi}(2-\epsilon)\arcsin\left(\frac{2-\epsilon}{2+\epsilon}\right). \tag{3.7}$$

For arbitrary dimensions we can expand the integral and obtain (to first order in ϵ) $G(\epsilon) = d - \frac{\epsilon}{2}$, such that for $U/J \to 0$ the rates (3.4) and (3.5) coincide.

2. Strong interactions

According to Eq. (3.1), the heating rate for a perfect Mott insulator with an integer number of atoms per site $\bar{n}$ is (to lowest order in J/U) given by

$$\frac{\langle\langle \dot{E} \rangle\rangle}{N} = S_0 \left(\frac{1}{J}\frac{dJ}{dV} - \frac{1}{U}\frac{dU}{dV} \right)^2 zUJ^2(\bar{n}+1). \tag{3.8}$$

Also here we can obtain corrections as well as insight into the excitation process by suitable approximations. Following [44] one can approximately describe the one-dimensional Bose-Hubbard model in the Mott regime by restricting the local Hilbert space to the three states $|\bar{n}\rangle$ and $|\bar{n} \pm 1\rangle$. Using a generalized Jordan-Wigner transformation one introduces fermionic creation operators for the excess particles ($c^\dagger_{j,+}$) and holes ($c^\dagger_{j,-}$). Assuming that the density of excess particles and holes is small, the Hamiltonian $H = H_J + H_U$ and the noise operator $H' = \frac{1}{J}\frac{dJ}{dV}H_J + \frac{1}{U}\frac{dU}{dV}H_U$ can be written in the quasimomentum basis approximately as

$$\begin{aligned} H_J &\approx -2J \sum_p \cos(pa)[(\bar{n}+1)c^\dagger_{p,+}c_{p,+} + \bar{n}c^\dagger_{p,-}c_{p,-}] \\ &\quad + \sqrt{\bar{n}(\bar{n}+1)}i \sin(pa)(c^\dagger_{p,+}c^\dagger_{-p,-} - c_{-p,-}c_{p,+}), \\ H_U &\approx U \sum_k \bar{n}c^\dagger_{p,+}c_{p,+} - (\bar{n}-1)c^\dagger_{p,-}c_{p,-}. \end{aligned} \tag{3.9}$$

The Hamiltonian H is then quadratic and can be diagonalized by the Bogoliubov transformation $\gamma^\dagger_{\sigma p,\sigma} = u_p c^\dagger_{p,\sigma} + v_p c_{\sigma p,\sigma}$, such that $H = \sum_{p,\sigma=\pm} \sigma\epsilon_\sigma(p)\gamma^\dagger_{p,\sigma}\gamma_{p,\sigma}$ with the quasiparticle dispersion relation

$$\epsilon_\pm(p) = -J\cos(pa) + \frac{U}{2}(2\bar{n}-1) \pm \frac{1}{2}\sqrt{[U - 2(2\bar{n}+1)J\cos(pa)]^2 + 16\bar{n}(\bar{n}+1)J^2\sin^2(pa)}. \tag{3.10}$$

As in the weakly interacting case, the noise operator H' is in general not diagonal in the quasiparticle basis, but it contains terms $\gamma^\dagger_{p,+}\gamma^\dagger_{-p,-}$ that generate correlated quasiparticle pairs that travel though the system with opposite quasimomentum. To lowest order in J/U, these are pairs of excess atoms and holes [Fig. 3(b)]. The heating rate associated with these processes can easily be calculated from (3.1) with (3.9) and (3.10) for the vacuum of quasiparticles. It is given by

$$\frac{\langle\langle \dot{E} \rangle\rangle}{N} = S_0 \left(\frac{1}{J}\frac{dJ}{dV} - \frac{1}{U}\frac{dU}{dV} \right)^2 2UJ^2(\bar{n}+1)F(J/U,\bar{n}), \tag{3.11}$$

where we abbreviated

$$\begin{aligned} F(j,n) &= \frac{1}{\pi}\int_0^\pi dp \frac{2\sin^2(p)}{\sqrt{f(j,n,p)}}, \\ f(j,n,p) &= [1-(4n+2)j\cos(p)]^2 + 16(n^2+n)j^2\sin^2(p). \end{aligned} \tag{3.12}$$

For $j \ll 1$ one finds $F(j,n) = 1 + (1-2n-2n^2)j^2 + O(j^4)$. For $J/U \to 0$ this reduces to (3.8).

3. Numerical results

In Fig. 4 we show results for the short-time mean heating rate per particle for unit filling ($\bar{n} = 1$) at different values for the interactions. The analytical results for weak and strong interaction are shown together with the results from numerical methods outlined in Sec. II C. The heating rates obtained with t-DMRG in one dimension (up to $N = M = 30$ particles per lattice site) agree very well with the analytical results in both limiting cases and connect these smoothly across the phase transition.

On a mean-field level the (ground state) phase transition from a SF ($|\psi_l|^2 > 0$) to an MI ($\psi_l = 0$) ground state occurs at $u_c \approx 5.8z$. The Gutzwiller wave function captures the two limiting cases of an ideal superfluid as a product of coherent states at each lattice site for vanishing interaction and a Mott insulator as a product of Fock states at each lattice site. However, a general limitation of the Gutzwiller mean-field theory is that the entire Mott insulating phase (at integer filling $\bar{n}$) is represented by the same wave function $|\Psi\rangle = \prod_l |\bar{n}\rangle_l$. This state is trivially invariant under the evolution with the stochastic equations (2.8). As an (unphysical) artifact of this limitation Eqs. (2.8) predict no heating in the entire Mott phase. The only nontrivial dynamics can be observed on the superfluid

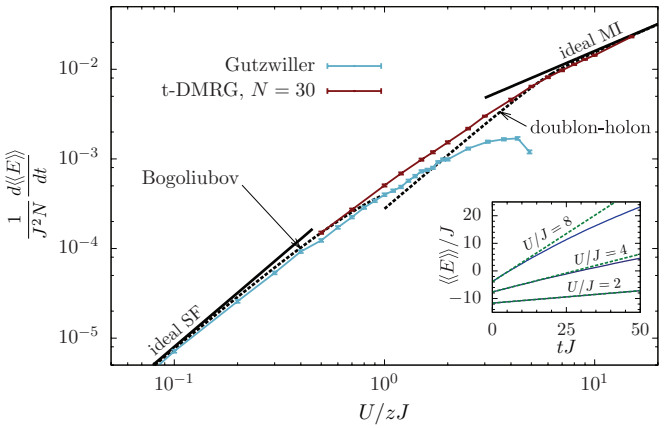

FIG. 4. (Color online) Comparison of the short-time heating rates from the Gutzwiller ansatz and t-DMRG simulations to the analytical results for weak and strong interactions. The Gutzwiller calculation is for a homogeneous infinite system, the DMRG simulation for a 1D system of 30 particles on 30 sites. We consider a small anticorrelated noise ($\sqrt{S}\frac{1}{J}\frac{dJ}{dV} = -0.01J^{-1/2}$, $\sqrt{S}\frac{1}{U}\frac{dU}{dV} = 0.01J^{-1/2}$). We average over $n_t = 1000$ ($n_t = 500$ for t-DMRG) noise trajectories and estimate statistical errors of the mean. Convergence has been checked with time steps $1 \times 10^{-3} \leqslant \Delta t J \leqslant 1 \times 10^{-2}$ and Hilbert space truncations $8 \leqslant d_l \leqslant 16$. The t-DMRG results are converged with a bond dimension of $D = 200$. The inset shows the averaged mean energy as a function of time (solid lines) together with the linear increase (dashed lines) with heating rate given by Eq. (3.1). This shows that the energy increase is well captured by a constant heating rate for several hopping times. The parameters and methods used to calculate the inset are the same as in Fig. 5(b).

side of the phase transition. On this side, except close to the phase transition, where the mean-field treatment is expected to fail, the results are in very good agreement with the analytical results obtained from the Bogoliubov approximation.

B. Evolution of state characteristics

The heating of a general many-body quantum state cannot be fully understood by a single heating rate, since the system is driven out of thermal equilibrium in general. In order to further quantify the heating, we analyze how characteristic correlation functions of the different many-body states are affected by the noisy lattice.

1. Single-particle density matrix and condensate fraction

For the Bose-Hubbard model, the MI and the SF states are characterized by the off-diagonal correlations, i.e., the off-diagonal elements of the single-particle density matrix (SPDM), $\langle b_i^\dagger b_{i+j}^\dagger \rangle$. The signature of the SF ground state is off-diagonal long-range order, i.e., these elements decay to a constant (decay algebraically in one dimension), whereas they decay exponentially to zero in the MI. Here we analyze how these characteristics change as a function of time.

Closely related to the SPDM is the condensate fraction, which is defined as the largest of the eigenvalues $\{\lambda_i\}$ of the SPDM: $\mathcal{F} \equiv \lambda_0/\sum_i \lambda_i$. Note that in the case of the Gutzwiller ansatz, the condensate fraction is simply given by $\mathcal{F} = |\psi_l|^2 = |\langle\phi_l|b_l|\phi_l\rangle|^2$. The perturbative analysis Sec. III A shows that the main effect of noise in the lattice depth on a Bose-Einstein condensate is the generation of quasiparticle pairs, and therefore a decrease of the number of atoms in the condensate mode with time. As for the heating rate one can calculate this depletion rate from the master equation (2.7). Denoting the number of atoms in the mode with quasimomentum q by $N_q \equiv \langle b_q^\dagger b_q\rangle$ we have $\langle\langle \dot{N}_q\rangle\rangle = \frac{S_0}{2}\xi\frac{1}{U}\frac{dU}{dV}\langle[[H_U, b_q^\dagger b_q], H_U]\rangle$ for the system initially in the ground state. In the limit of an ideal condensate the number of atoms in the condensate mode at $q = 0$ evaluates to $\langle\langle \dot{N}_0\rangle\rangle/N_0 = -S_0\xi\frac{1}{U}\frac{dU}{dV}U^2\frac{N_0}{M}$. Within the same approximation the quasimomentum of the particles scattered out of the condensate mode is distributed homogeneously over the whole Brillouin zone: $\langle\langle \dot{N}_q\rangle\rangle = S_0\xi\frac{1}{U}\frac{dU}{dV}U^2\frac{N_0^2}{M^2}$.

Numerical solutions of the stochastic differential equation show such a depletion of the condensate mode, both using exact methods [Figs. 5(a), 5(b), and Fig. 6] (exact diagonalization and t-DMRG) as well as in the Gutzwiller framework [Fig. 5(c)]. By performing a small noise expansion [33] of the nonlinear stochastic Gutzwiller equations we find that this initial decay of the condensate fraction in the Gutzwiller framework is associated with the incoherent excitation of the amplitude mode at zero quasimomentum [43] [see Fig. 5(c)]. However, we note that for long times solutions to the

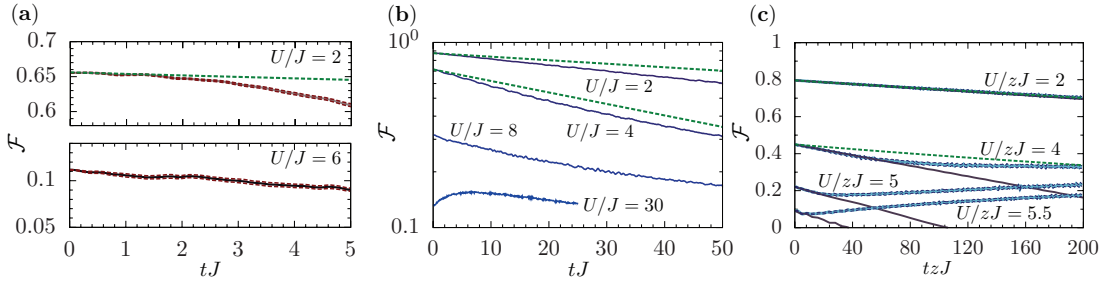

FIG. 5. (Color online) (a) The time evolution of the condensate fraction for short times in a large system with $M = N = 48$ (averaged over 60 trajectories, bond dimension $D = 256$, local dimension truncation $d_l = 6$), (b) for long times in a small system with $N = M = 10$ (500 trajectories), and (c) for a homogeneous infinite Bose-Hubbard model in mean-field theory (Gutzwiller ansatz, $d_l = 8$, 1000 trajectories, solid grey lines obtained by a small noise approximation [33]). The fraction in general decreases except for the extreme Mott insulating case of $U/J = 30$ and in the long-time limit in mean-field theory. In (a) the noise is anticorrelated with $\sqrt{S}\frac{1}{J}\frac{dJ}{dV} = -0.025J^{-1/2}$, $\sqrt{S}\frac{1}{U}\frac{dU}{dV} = 0.025J^{-1/2}$, in (c) with $\sqrt{S}\frac{1}{J}\frac{dJ}{dV} = -0.01J^{-1/2}$, $\sqrt{S}\frac{1}{U}\frac{dU}{dV} = 0.01J^{-1/2}$. In all three plots, the straight dashed green lines correspond to the result obtained in perturbation theory (see text).

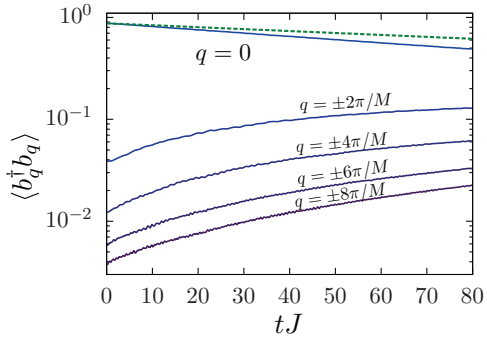

FIG. 6. (Color online) The evolution of the population in different quasimomentum modes. Shown are averages over 500 noise realizations for a superfluid state ($U/J = 2$) for a 1D system with $N = 10$ particles on $M = 10$ sites. The lattice fluctuations lead to a decrease of the population in the condensate mode at $q = 0$ in agreement with the prediction from perturbation theory given by the dashed line. The noise is anticorrelated with $\sqrt{S}\frac{1}{J}\frac{dJ}{dV} = -0.025J^{-1/2}$, $\sqrt{S}\frac{1}{U}\frac{dU}{dV} = 0.025J^{-1/2}$.

Gutzwiller equations (2.8) have a mean condensate fraction of approximately ∼0.3. This steady-state mean condensate fraction is not associated with a steady-state condensate fraction in the individual trajectory, where in the long-time limit the condensate fraction oscillates between 0 and 1 with a random phase, which gives rise to a nonzero steady-state behavior for the stochastic average. Such a signature is considered an unphysical artifact of the incapacity of the Gutzwiller wave function to capture the decay of the amplitude mode. In fact, exact simulations of one-dimensional systems show no such behavior.

In Fig. 5(b), we show the stochastic average of the condensate fraction for a 1D system of ten sites and periodic boundary conditions using exact diagonalization. Even though in one dimension the ground state shows only quasi-long-range order, for small values of U/J the decay of the condensate fraction is well described by the expression obtained in perturbation theory. Our t-DMRG simulations essentially lead to the same results but are limited to very short times [Fig. 5(a)]. In contrast to the Gutzwiller results, the condensate fraction decreases monotonically also for long times for all superfluid initial states.

2. *Particle-hole correlations*

In the limit of strong interactions, as shown above, we expect elementary excitations to consist of correlated particle-hole pairs propagating through the system. To analyze the dynamics associated with these excitations, we compute parity correlation functions defined as [44]

$$C_l^{[i]} = \langle s_i s_{i+l} \rangle - \langle s_i \rangle \langle s_{i+l} \rangle, \tag{3.13}$$

where s_j is the local parity operator at site j, defined as $s_j = \exp\{i\pi(n_j - \bar{n})\}$. Since we calculate these functions in finite inhomogeneous 1D systems, $C_l^{[i]}$ depends on the site i from which we start calculating the function, and we will typically begin from the central site $i = M/2$ in a system of M sites. In Fig. 7 we plot the evolution of this correlation function under the evolution with the SMBSE, calculated with t-DMRG for a

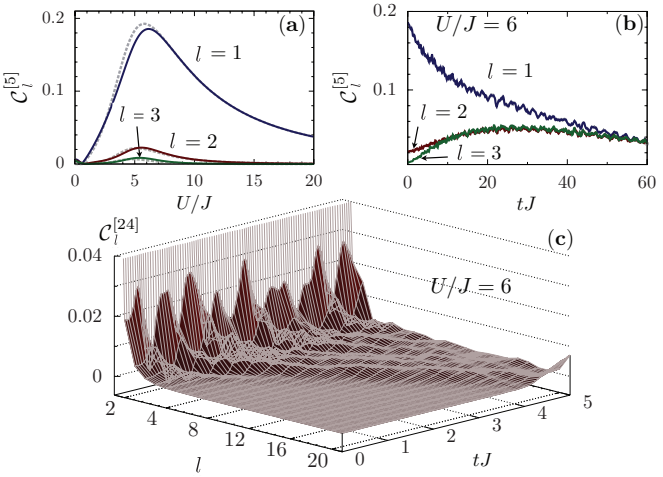

FIG. 7. (Color online) (a) Parity correlations in the ground state of a small system with $N = M = 10$. The next-neighbor and longer-ranged correlations assume a maximum at $U/J \approx 6$ (solid lines are for open, dashed lines are for periodic boundary conditions). (b) Long-time evolution of these correlations calculated with exact diagonalization in the small system, averaged over 500 noise trajectories (periodic boundary conditions). The transient state develops long-range correlations. (c) The evolution of the parity-parity correlation function of a single noise trajectory in a Mott insulating state with $U/J = 6$ in a 1D system with $N = M = 48$ (bond dimension $D = 265$, local dimension truncation $d_l = 6$). The amplitude noise excites single particle-hole pairs which spread out through the system as a light cone. In all simulations, the noise is anticorrelated with $\sqrt{S}\frac{1}{J}\frac{dJ}{dV} = -0.025J^{-1/2}$, $\sqrt{S}\frac{1}{U}\frac{dU}{dV} = 0.025J^{-1/2}$.

large system and with exact diagonalization for a small system. Note that useful information about these correlations cannot be obtained from a Gutzwiller product state ansatz, as the first term of (3.13) will always factorize and thus the correlation will always be zero.

As seen in Fig. 7(a), the parity correlations in the ground state assume the largest value in the Mott insulating phase at $U/J \approx 6$. In a noisy time evolution we find that the initially large next-neighbor parity correlation starts to decrease, whereas the long-range parity correlations start to increase, as shown in Fig. 7(b). It reaches a maximum at a transient state at times $tJ \approx 30$, where the next-neighbor and long-range interactions assume nearly the same value. At longer times all these correlations start to decrease into a more and more classical state without correlations. Furthermore, looking at a single noise trajectory in a large system, we find in Fig. 7(c) that the elementary excitations induced by the amplitude noise are seen as excitations in the parity-parity correlations, which spread out in the form of a light cone, similar to the results in [44], where these correlation functions are directly measured in a quantum gas microscope experiment.

IV. SUMMARY AND OUTLOOK

In conclusion we have derived a microscopic model for the dynamics of bosonic atoms in a time-dependent optical lattice. While controlled periodic modulation of the lattice has the potential to access interesting physics [29,30], we considered the alternative situation where the lattice depth fluctuates

stochastically at low frequency. This situation arises naturally in optical lattice experiments due to intensity fluctuations of the lattice lasers. Using analytical approximations as well as t-DMRG and time-dependent Gutzwiller methods, we have analyzed the nonequilibrium dynamics of many-body states in a variety of parameter regimes. We find characteristic responses of the system that vary in different parameter regimes, and could be used to identify the effects of such dynamics in current experiments.

The generalization of the initial model to fermionic atoms results in a stochastic equation of motion similar to (2.6),

$$(S) \quad d|\Psi\rangle = -iH|\Psi\rangle dt - iH'\sqrt{S_0}|\Psi\rangle dW_t, \tag{4.1}$$

with a coherent part given by the Fermi-Hubbard Hamiltonian, and a corresponding stochastic contribution:

$$H = -J\sum_{\langle i,j\rangle,\sigma} c^\dagger_{i,\sigma}c_{j,\sigma} + U\sum_i c^\dagger_{i,\uparrow}c_{i,\uparrow}c^\dagger_{i,\downarrow}c_{i,\downarrow}, \tag{4.2}$$

$$H' = -\frac{dJ}{dV}\sum_{\langle i,j\rangle,\sigma} c^\dagger_{i,\sigma}c_{j,\sigma} + \frac{dU}{dV}\sum_i c^\dagger_{i,\uparrow}c_{i,\uparrow}c^\dagger_{i,\downarrow}c_{i,\downarrow}. \tag{4.3}$$

Here the $c_{i,\sigma}$ are operators annihilating a fermion at site i with spin $\sigma \in \{\uparrow,\downarrow\}$. An analysis of this equation, similar to the one presented in Sec. III, can be carried out. In the Mott insulator at half filling for the antiferromagnetic ground state ($U \gg J$) a heating rate of $\dot{E}/N = S_0\xi^2 U z J^2$ can be found from mean-field calculations. Exploration of heating in other regimes, e.g., in the BCS-BEC crossover, is an interesting direction for further analysis.

ACKNOWLEDGMENTS

We thank P. Barmettler, S. Blatt, M. Lukin, C. Spee, and the groups of I. Bloch and W. Ketterle for helpful and motivating discussions. H.P. thanks the University of Pittsburgh for hospitality. This work was supported in part by the Austrian Science Fund through SFB F40 FOQUS, and by a grant from the US Army Research Office with funding from the DARPA OLE program. Work in Pittsburgh was supported by AFOSR Grant No. FA9550-12-1-0057, and computational resources were provided by the Center for Simulation and Modeling at the University of Pittsburgh.

APPENDIX: INTERBAND TRANSITIONS

Here we comment on the derivation of the SMBSE focusing on the transitions to higher bands due to nonadiabatic transitions.

To proceed from Eq. (2.3) we expand the field operator in the instantaneous Wannier basis. The coefficients of the wave function $|\Psi\rangle$ in the corresponding instantaneous Fock basis $|\{n_{i,n}\}\rangle$ change in time via the change of the wave function and via the change of the time-dependent basis states:

$$\frac{d}{dt}\langle\{n_{i,n}\}|\Psi\rangle = \left(\frac{d}{dt}\langle\{n_{i,n}\}|\right)|\Psi\rangle + \langle\{n_{i,n}\}|\left(\frac{d}{dt}|\Psi\rangle\right). \tag{A1}$$

The time derivative of a Fock basis state $|\{n_{i,n}\}\rangle$ constructed from the time-dependent single-particle basis $w_{i,n}(x,V(t))$ can be obtained from the time derivative of the corresponding annihilation operators: $b_{i,n} = \int dx\, w_{i,n}(x,V(t))\hat{\psi}(x)$. With $\psi(x) = \sum_{i,n} w_{i,n}(x,V(t))b_{i,n}$ we find

$$\frac{d}{dt}b_{i,n} = \sum_{i,n}\int dx\left(\frac{d}{dt}w_{i,n}(x,V(t))\right)w_{i,n}(x,V(t))b_{i,n}. \tag{A2}$$

This expresses the change of the annihilation operators in the Schrödinger picture due to the change of the basis states. It should not be confused with the Heisenberg equation of motion for this operators. With this relation it is easy to show that the corresponding Fock states $|\{n_{i,n}\}\rangle$ change due to the changing single-particle basis as

$$\frac{d}{dt}|\{n_{i,n}\}\rangle = \sum_{r,s,j,m}\int dx\, w_{j,m}(x,V(t)) \times\left(\frac{d}{dt}w_{r,s}(x,V(t))\right)b^\dagger_{j,m}b_{r,s}|\{n_{i,n}\}\rangle, \tag{A3}$$

which gives rise to the term $G(V(t))$ in Eq. (2.5). A similar derivation is given in [31]. To see that this term couples only states in different bands it is instructive to transform $G(V)$ to the instantaneous Bloch basis $\phi_{q,n}(x,V)$ (with the corresponding annihilation operator $b_{q,n}$),

$$G(V) = i\sum_{q,n;p,m}\int dx\,\phi_{p,m}(x,V)\frac{d\phi^*_{q,n}(x,V)}{dV}b^\dagger_{q,n}b_{p,m}. \tag{A4}$$

The derivative of the Bloch state $\phi_{q,n}(x,V)$ with respect to the lattice depth can be expressed in terms of the Bloch states with the same quasimomentum q, but in different bands $m \neq n$. From first-order perturbation theory we find

$$\frac{d}{dV}\phi_{q,n}(x,V) = \sum_{m\neq n}\phi_{q,m}(x,V)\sigma_{q,m}(V), \tag{A5}$$

$$\sigma_{q,m}(V) = \frac{\int dy\,\phi^*_{q,m}(y,V)\phi_{q,n}(y,V)\sin^2(ky)}{\varepsilon_{q,n}(V) - \varepsilon_{q,m}(V)}. \tag{A6}$$

Thus the integral in (A4) is nonzero only for $p = q$ and for $n \neq m$. The operator $G(V)$ therefore transfers single atoms into a different band with the same quasimomentum. This conservation of quasimomentum reflects the fact that the lattice translation symmetry is not broken by global fluctuations in the lattice depth. Further, the perturbation does not break the reflection symmetry $x \to -x$. As a consequence, bands with even (odd) band index n are coupled only to bands with an even (odd) band index m.

To lowest order in $J/|\omega_{n,m}|$, with $\omega_{n,m}$ being the energy difference between the bands n and m, we can find a simple expression for the resonant parts in $G(V_0)\delta\dot{V}(t)$ that affect atoms in the lowest band:

$$G(V_0)\delta\dot{V}(t) \approx \sum_{i,n>0}\lambda_{i,n}\delta V_n(t)b^\dagger_{i,n}b_{i,0} + \text{H.c.}, \tag{A7}$$

$$\lambda_{i,n} = \int dx\, w_{i,n}(x)\sin^2(kx)w_{i,0}(x), \tag{A8}$$

where we again kept only terms diagonal in the site index i due to the localized form of the Wannier functions. Here $\delta V_n(t)$ denotes restriction of the noise term $\delta V(t)$ to frequencies around transition frequency from the lowest to the nth band. Approximating the Wannier functions at a given lattice site with harmonic oscillator wave functions, we find that atoms

in the lowest band are dominantly scattered into the second excited band in such band-changing processes. To lowest order in the Lamb-Dicke parameter $\eta = ka_0$, which measures the extension of the Wannier function a_0, compared to the lattice constant $a = \pi/k$, one finds $\lambda_{i,n} \approx \sqrt{2}\eta^2\delta_{n,2} + O(\eta^4)$. Thus, the number of atoms in the lowest band N_0 decreases in time as $\dot{N}_0/N_0 = -\sum_{n>0} S_n\lambda_{i,n}^2 \approx -2\eta^4 S_2$. This sets the time scale on which the restriction to the lowest band is valid.

[1] I. Bloch, J. Dalibard, and W. Zwerger, Rev. Mod. Phys. **80**, 885 (2008).

[2] M. Lewenstein, A. Sanpera, and V. Ahufinger, *Ultracold Atoms in Optical Lattices: Simulating Quantum Many-body Systems* (Oxford University Press, New York, 2012).

[3] D. Jaksch and P. Zoller, Ann. Phys. **315**, 52 (2005).

[4] M. Greiner, O. Mandel, T. Esslinger, T. W. Hänsch, and I. Bloch, Nature (London) **415**, 39 (2002).

[5] U. Schneider, L. Hackermüller, S. Will, Th. Best, I. Bloch, T. A. Costi, R. W. Helmes, D. Rasch, and A. Rosch, Science **322**, 1520 (2008).

[6] E. Haller, M. Gustavsson, M. J. Mark, J. G. Danzl, R. Hart, Pupillo, and H.-C. Nägerl, Science **325**, 1224 (2009).

[7] R. Jördens, L. Tarruell, D. Greif, T. Uehlinger, N. Strohmaier, H. Moritz, T. Esslinger, L. De Leo, C. Kollath, A. Georges, V. Scarola, L. Pollet, E. Burovski, E. Kozik, and M. Troyer, Phys. Rev. Lett. **104**, 180401 (2010).

[8] S. Nascimbene, N. Navon, K. J. Jiang, F. Chevy, and C. Salomon, Nature (London) **463**, 1057 (2010).

[9] P. Soltan-Panahi, D.-S. Lühmann, J. Struck, P. Windpassinger, and K. Sengstock, Nat. Phys. **8**, 71 (2012).

[10] X. Zhang, C.-L. Hung, S.-K. Tung, and C. Chin, Science **335**, 1070 (2012).

[11] M. J. H. Ku, A. T. Sommer, L. W. Cheuk, and M. W. Zwierlein, Science **335**, 6068 (2012).

[12] J. Simon, W. S. Bakr, R. Ma, M. E. Tai, P. M. Preiss, and M. Greiner, Nature (London) **472**, 307 (2011).

[13] J. I. Cirac and P. Zoller, Nat. Phys. **8**, 264 (2012).

[14] I. Bloch, J. Dalibard and S. Nascimbne, Nat. Phys. **8**, 267 (2012).

[15] S. Trotzky, Y-A. Chen, A. Flesch, I. P. McCulloch, U. Schollwöck, J. Eisert, and I. Bloch, Nat. Phys. **8**, 325 (2012).

[16] H. Pichler, A. J. Daley, and P. Zoller, Phys. Rev. A **82**, 063605 (2010).

[17] D. Poletti, J.-S. Bernier, A. Georges, and C. Kollath, arXiv:1212.4254.

[18] S. Trotzky, L. Pollet, F. Gerbier, U. Schnorrberger, I. Bloch, N. Prokofiev, B. Svistunov, and M. Troyer, Nat. Phys. **6**, 998 (2010).

[19] F. Gerbier and Y. Castin, Phys. Rev. A **82**, 013615 (2010).

[20] K. Günter, T. Stöferle, H. Moritz, M. Köhl, and T. Esslinger, Phys. Rev. Lett. **96**, 180402 (2006).

[21] N. Syassen, D. M. Bauer, M. Lettner, T. Volz, D. Dietze, J. J. Garca-Ripoll, J. I. Cirac, G. Rempe, and S. Dürr, Science **320**, 5881 (2008).

[22] A. J. Daley, J. M. Taylor, S. Diehl, M. Baranov, and P. Zoller, Phys. Rev. Lett. **102**, 040402 (2009).

[23] See, e.g., A. Liem, J. Limpert, H. Zellmer, and A. Tünnermann, Opt. Lett. **28**, 1537 (2003).

[24] H. Pichler, J. Schachenmayer, J. Simon, P. Zoller, and A. J. Daley, Phys. Rev. A **86**, 051605(R) (2012).

[25] D. Jaksch, C. Bruder, J. I. Cirac, C. W. Gardiner, and P. Zoller, Phys. Rev. Lett. **81**, 3108 (1998).

[26] T. Stöferle, H. Moritz, C. Schori, M. Köhl, and T. Esslinger, Phys. Rev. Lett. **92**, 130403 (2004).

[27] A. Iucci, M. A. Cazalilla, A. F. Ho, and T. Giamarchi, Phys. Rev. A **73**, 041608(R) (2006).

[28] C. Kollath, A. Iucci, T. Giamarchi, W. Hofstetter, and U. Schollwöck, Phys. Rev. Lett. **97**, 050402 (2006).

[29] D. Greif, L. Tarruell, T. Uehlinger, R. Jördens, and T. Esslinger, Phys. Rev. Lett. **106**, 145302 (2011).

[30] A. Tokuno and T. Giamarchi, Phys. Rev. Lett. **106**, 205301 (2011).

[31] M. Lacki and J. Zakrzewski, Phys. Rev. Lett. **110**, 065301 (2013).

[32] P. E. Koeden and P. Platen, *Numerical Solution of Stochastic Differential Equations*, Applications of Mathematics, Stochastic Modelling and Applied Probability, Vol. 23 (Springer-Verlag, Berlin 1992).

[33] C. W. Gardiner, *Stochastic Methods*, Springer Series in Synergetics (Springer-Verlag, Berlin, 2009).

[34] G. Vidal, Phys. Rev. Lett. **91**, 147902 (2003).

[35] G. Vidal, Phys. Rev. Lett. **93**, 040502 (2004).

[36] A. J. Daley, C. Kollath, U. Schollwöck, and G. Vidal, J. Stat. Mech. (2004) P04005.

[37] S. R. White and A. E. Feiguin, Phys. Rev. Lett. **93**, 076401 (2004).

[38] M. P. A. Fisher, P. B. Weichman, G. Grinstein, and D. S. Fisher, Phys. Rev. B **40**, 546 (1989).

[39] D. S. Rokhsar and B. G. Kotliar, Phys. Rev. B **44**, 10328 (1991).

[40] W. Krauth, M. Caffarel, and J.-P. Bouchaud, Phys. Rev. B **45**, 3137 (1992).

[41] D. Jaksch, V. Venturi, J. I. Cirac, C. J. Williams, and P. Zoller, Phys. Rev. Lett. **89**, 040402 (2002).

[42] J. Zakrzewski, Phys. Rev. A **71**, 043601 (2005).

[43] K. V. Krutitsky and P. Navez, Phys. Rev. A **84**, 033602 (2011).

[44] M. Cheneau, P. Barmettler, D. Poletti, M. Endres, P. Schauß, T. Fukuhara, C. Gross, I. Bloch, C. Kollath, and S. Kuhr, Nature (London) **481**, 484 (2012).